The Astrophysical Journal, 670:826–832, 2007 November 20

HD 147506b: A SUPERMASSIVE PLANET IN AN ECCENTRIC ORBIT TRANSITING A BRIGHT STAR[1]

G. Á. Bakos,[2,3] G. Kovács,[4] G. Torres,[2] D. A. Fischer,[5] D. W. Latham,[2] R. W. Noyes,[2] D. D. Sasselov,[2] T. Mazeh,[6] A. Shporer,[6] R. P. Butler,[7] R. P. Stefanik,[2] J. M. Fernández,[2] A. Sozzetti,[2,8] A. Pál,[9,2] J. Johnson,[10] G. W. Marcy,[10] J. N. Winn,[11] B. Sipőcz,[9,2] J. Lázár,[12] I. Papp,[12] and P. Sári[12]

Received 2007 April 29; accepted 2007 July 20

ABSTRACT

We report the discovery of a massive ($M_p = 9.04 \pm 0.50\ M_J$) planet transiting the bright ($V = 8.7$) F8 star HD 147506, with an orbital period of 5.63341 ± 0.00013 days and an eccentricity of $e = 0.520 \pm 0.010$. From the transit light curve we determine that the radius of the planet is $R_p = 0.982^{+0.038}_{-0.105}\ R_J$. HD 147506b (also coined HAT-P-2b) has a mass about 9 times the average mass of previously known transiting exoplanets and a density of $\rho_p \approx 12$ g cm^{-3}, greater than that of rocky planets like the Earth. Its mass and radius are marginally consistent with theories of structure of massive giant planets composed of pure H and He, and accounting for them may require a large ($\gtrsim 100\ M_\oplus$) core. The high eccentricity causes a ninefold variation of insolation of the planet between peri- and apastron. Using follow-up photometry, we find that the center of transit is $T_{\rm mid} = 2{,}454{,}212.8559 \pm 0.0007$ (HJD) and the transit duration is 0.177 ± 0.002 days.

Subject headings: planetary systems — stars: individual (HD 147506)

On-line material: color figure, machine-readable table

1. INTRODUCTION

To date 18 extrasolar planets have been found that transit their parent stars and thus yield values for their mass and radius.[13] Masses range from 0.3 to about 1.9 M_J, and radii from 0.7 to about 1.4 R_J. The majority fit approximately what one expects from theory for irradiated gas giant planets (e.g., Fortney et al. 2007 and references therein, hereafter FMB07), although there are exceptions: HD 149026b has a small radius for its mass (Sato et al. 2005), implying that it has a large heavy core ($\sim 70\ M_\oplus$; Laughlin et al. 2005), and several (HD 209458b, HAT-P-1b, WASP-1) have unexpectedly large radii for their masses, perhaps suggesting some presently unknown source of extra internal heating (Guillot & Showman 2002; Bodenheimer et al. 2003). The longest period and lowest density transiting exoplanet (TEP) detected so far is HAT-P-1b, with $P = 4.46$ days (Bakos et al. 2007). All TEPs have orbits consistent with circular Keplerian motion.

From existing radial velocity (RV) data, it might be expected that there are some close-in (semimajor axis $\lesssim 0.07$ AU, or $P \lesssim 10$ days) giant planets with masses considerably larger than any of the 18 transiting planets now known. A well-known example, considering only objects below the deuterium burning threshold (~ 13; e.g., Burrows et al. 1997), is τ Boo b, which was detected from RV variations, has a minimum mass of $M_p \sin i = 3.9\ M_J$, and orbits only 0.046 AU from its star (Butler et al. 1997). Another example is HIP14810b (Wright et al. 2007) with similar mass an orbital period of 6.7 days, and semimajor axis of 0.069 AU. At this orbital distance the a priori probability of such a planet transiting its star is about 10%. Thus, "supermassive" planets should sometimes be found transiting their parent stars. We report here the detection of the first such TEP and our determination of its mass and radius. This is also the longest period TEP and the first one to exhibit highly eccentric orbit.

2. OBSERVATIONS AND ANALYSIS

2.1. *Detection of the Transit in the HATNet Data*

HD 147506 is an F8 star with visual magnitude 8.7 and *Hipparcos* parallax 7.39 ± 0.88 mas (Perryman et al. 1997). It was initially identified as a transit candidate in our internally labeled field G193 in the data obtained by HATNet's[14] (Bakos et al. 2002, 2004) HAT-6 telescope at the Fred Lawrence Whipple Observatory (FLWO) of the Smithsonian Astrophysical Observatory (SAO). The detection of a ~ 5 mmag transit with a 5.63 day period in the light curve consisting of ~ 7000 data points (with a 5.5 minute cadence) was marginal. Fortunately, the star was in the overlapping corner with another field (G192) that has been jointly observed by HATNet's HAT-9 telescope at the Submillimeter Array (SMA) site atop Mauna Kea, Hawaii, and by the Wise HAT telescope

[1] Some of the data presented herein were obtained at the W. M. Keck Observatory, which is operated as a scientific partnership among the California Institute of Technology, the University of California, and the National Aeronautics and Space Administration. The Observatory was made possible by the generous financial support of the W. M. Keck Foundation. The authors wish to recognize and acknowledge the very significant cultural role and reverence that the summit of Mauna Kea has always had within the indigenous Hawaiian community. We are most fortunate to have the opportunity to conduct observations from this mountain. Keck time has been in part granted by NASA.

[2] Harvard-Smithsonian Center for Astrophysics, 60 Garden Street, Cambridge, MA 02138; gbakos@cfa.harvard.edu.

[3] Hubble Fellow.

[4] Konkoly Observatory, Budapest, P.O. Box 67, H-1125, Hungary.

[5] Department of Physics and Astronomy, San Francisco State University, San Francisco, CA 94132.

[6] Wise Observatory, Tel Aviv University, Tel Aviv, Israel 69978.

[7] Department of Terrestrial Magnetism, Carnegie Institute of Washington DC, 5241 Broad Branch Road, NW, Washington DC, 20015-1305.

[8] INAF–Osservatorio Astronomico di Torino, Strada Osservatorio 20, 10025 Pino Torinese, Italy.

[9] Department of Astronomy, Eötvös Loránd University, Pf. 32, H-1518 Budapest, Hungary.

[10] Department of Astronomy, University of California, Berkeley, CA 94720.

[11] Department of Physics, and Kavli Institute for Astrophysics and Space Research, Massachusetts Institute of Technology, Cambridge, MA 02139.

[12] Hungarian Astronomical Association, P. O. Box 219, 1461 Budapest, Hungary.

[13] See The Extrasolar Planets Encyclopedia at http://exoplanet.eu.

[14] At http://www.hatnet.hu.

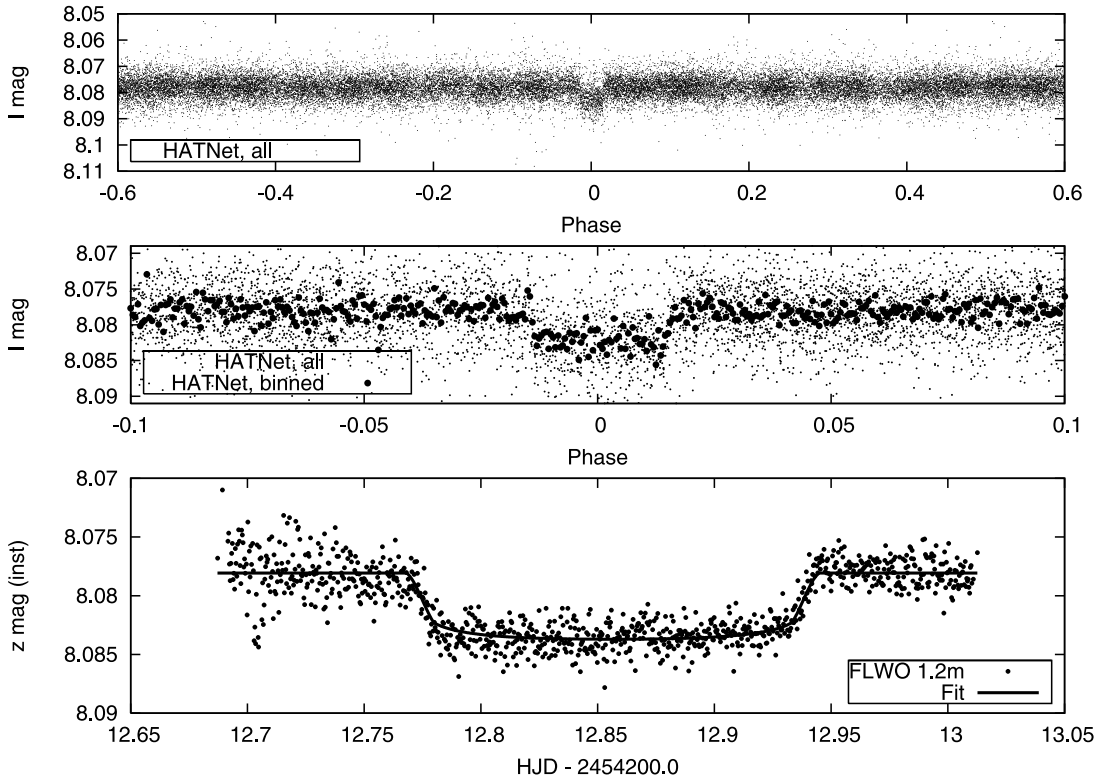

FIG. 1.—*Top*: Unbinned HATNet and WHAT joint light curve with 26,400 data points, phased with the $P = 5.63341$ day period. The 5 mmag deep transit is detected with a S/N of 26. *Middle*: Same HATNet and WHAT data zooming in on the transit and binned with a $\phi = 0.0005$ bin-size. *Bottom*: Sloan z-band photometry taken with the FLWO 1.2 m telescope. Overplotted is our best fit obtained with the Mandel & Agol (2002) formalism.

(WHAT; Wise Observatory, Israel; Shporer et al. 2006) for an extended period that yielded ~6700 and ~3900 additional data points, respectively. The transit was independently detected and confirmed with these data sets. By chance, the candidate is in yet another joint field (G149) of HATNet (HAT-7 at FLWO) and WHAT, contributing ~6200 and ~2200 additional data points, respectively. Altogether this resulted in a light curve with exceptional time coverage (570 days), an unprecedented number of data points (26,461 measurements at 5.5 minute cadence), and an rms of 5 mmag. It is noteworthy that the network coverage by WHAT (longitude E35°), HATNet at FLWO (W111°) and HATNet at Hawaii (W155°) played an important role in detecting such a long period and shallow transit. Data were reduced using astrometry from Pál & Bakos (2006) and with a highly fine tuned aperture photometry. We applied our external parameter decorrelation (EPD) technique on the light curves, whereby deviations from the median were cross-correlated with a number of "external parameters," such as the X and Y subpixel position, hour angle, and zenith distance. We have also applied the trend-filtering algorithm (TFA; Kovács et al. 2005, hereafter KBN05) along with the box least-squares (BLS; Kovács et al. 2002) transit-search algorithm in our analysis. TFA and BLS were combined in signal-reconstruction mode, assuming general signal shape, as described in KBN05. The detection of this relatively shallow transit is a good demonstration of the strengths of TFA. The top panel of Figure 1 shows the unbinned light curve with all 26,400 data points, whereas the middle panel displays the transit binned to 1/2000 of the period (4 minutes). We note that due to the large amount of data, the binned light curve is of similar precision as a single-transit observation by a 1 m class telescope.

After several failed attempts (due to bad weather and instrument failure) to carry out high-precision photometric follow-up observations from FLWO, Wise Observatory, Konkoly Observatory, and the Clay Center (Boston), we finally succeeded in observing a full transit using the KeplerCam detector on the FLWO 1.2 m telescope (see Holman et al. 2007) on UT 2007 April 22. The Sloan z-band light curve is shown in the bottom panel of Figure 1. From the combined HATNet and KeplerCam photometry, spanning a baseline of 839 days, we derive a period of 5.63341 ± 0.00013 days and an epoch of midtransit of $T_{\rm mid} = 2{,}454{,}212.8559 \pm 0.0007$ days (HJD). From the FLWO 1.2 m data alone (and the analytic light curve fit as described below), the length of transit is 0.177 ± 0.002 days (4 hr, 15 minutes), the length of ingress is 0.012 ± 0.002 days (17.5 minutes), and the depth (at the middle of the transit) is 0.0052 mag.

2.2. *Early Spectroscopy Follow-up*

Initial follow-up observations were made with the CfA Digital Speedometer (DS; Latham 1992) in order to characterize the host star and to reject obvious astrophysical false-positive scenarios that mimic planetary transits. These observations yielded values of $T_{\rm eff} = 6250$ K, $\log g = 4.0$, and $v \sin i = 22$ km s^{-1}, corresponding to a moderately rotating main-sequence F star. The radial velocity (RV) measurements showed an rms residual of ~0.82 km s^{-1}, slightly larger than the nominal DS precision for a star with this rotation, and suggested that they may be variable. With a few dozen additional DS observations, it was found that the RV appeared periodic, with $P \approx 5.63$ days, semiamplitude ~1 km s^{-1}, and phasing in agreement with predictions from the HATNet+WHAT light curve. This gave strong evidence that there really was an RV signal resulting from Keplerian motion, although the precision was insufficient to establish the orbit with confidence. Altogether, we collected 53 individual spectra spanning a time base of more than a year (Table 1).

TABLE 1
Radial Velocities for HD 147506

BJD −2,400,000 (days)	RV[a] (m s^{-1})	Uncertainty (m s^{-1})	Observatory[b]
53,981.7775.....	−556.0	8.4	Keck
53,982.8717.....	−864.1	8.5	Keck
53,983.8148.....	−62.9	8.8	Keck
53,984.8950.....	280.6	8.6	Keck
54,023.6915.....	157.8	9.9	Keck
54,186.9982.....	120.2	5.5	Keck
54,187.1041.....	104.6	5.7	Keck
54,187.1599.....	130.1	5.3	Keck
54,188.0169.....	168.5	5.3	Keck
54,188.1596.....	198.2	5.5	Keck
54,189.0104.....	68.9	5.7	Keck
54,189.0889.....	69.7	6.2	Keck
54,189.1577.....	25.2	6.1	Keck
54,168.9679.....	−152.7	42.1	Lick
54,169.9519.....	542.4	41.3	Lick
54,170.8619.....	556.8	42.6	Lick
54,171.0365.....	719.1	49.6	Lick
54,218.8081.....	−1165.2	88.3	Lick
54,218.9856.....	−1492.6	90.8	Lick
54,219.9373.....	−28.2	43.9	Lick
54,219.9600.....	−14.8	43.9	Lick
54,220.9641.....	451.6	38.4	Lick
54,220.9934.....	590.7	37.1	Lick

Note.—Table 1 is published in its entirety in the electronic edition of the *Astrophysical Journal*. A portion is shown here for guidance regarding its form and content.

[a] The RVs include the barycentric correction.

[b] Only the Keck and Lick data points are shown here. Consult the electronic edition for a full data set that includes the CfA DS measurements.

2.3. *High-Precision Spectroscopy Follow-up*

In order to confirm or refute the planetary nature of the transiting object, we pursued follow-up observations with the HIRES instrument (Vogt et al. 1994) on the W. M. Keck telescope and with the Hamilton echelle spectrograph at the Lick Observatory (Vogt 1987). The spectrometer slit used at Keck is 0.86″, yielding a resolving power of about 55,000 with a spectral coverage between about 3200″ and 8800 Å. The Hamilton echelle spectrograph at Lick has a similar resolution of about 50,000. These spectra were used (1) to more fully characterize the stellar properties of the system, (2) to obtain a radial velocity orbit, and (3) to check for spectral line bisector variations that may be indicative of a blend. We gathered 13 spectra at Keck (plus an iodine-free template) spanning 207 days and 10 spectra at Lick (plus template) spanning 50 days. The radial velocities measured from these spectra are shown in Table 1, along with those from the CfA DS.

3. STELLAR PARAMETERS

A spectral synthesis modeling of the iodine-free Keck template spectrum was carried out using the SME software (Valenti & Piskunov 1996), with the wavelength ranges and atomic line data described by Valenti & Fischer (2005). Results are shown in Table 2. The values obtained for the effective temperature ($T_{\rm eff}$), surface gravity ($\log g$), and projected rotational velocity ($v \sin i$) are consistent with those found from the CfA DS spectra. As a check on $T_{\rm eff}$, we collected all available photometry for HD 147506 in the Johnson, Cousins, 2MASS, and Tycho systems, and applied a number of color-temperature calibrations (Ramírez & Meléndez 2005; Masana et al. 2006; Casagrande et al. 2006) using seven different color indices. These resulted in an average temperature of $\sim$6400 $\pm$ 100 K, somewhat higher than the spectroscopic value, but consistent within the errors.

TABLE 2
Summary of Stellar Parameters for HD 147506

Parameter	Value	Source
$T_{\rm eff}$ (K).....	6290 $\pm$ 110	SME
$\log g$	4.22 $\pm$ 0.14	SME
$v \sin i$ (km s^{-1}).....	19.8 $\pm$ 1.6	SME
[Fe/H] (dex).....	+0.12 $\pm$ 0.08	SME
Distance (pc)	135 $\pm$ 16	HIP
Distance (pc)	110 $\pm$ 15	Y^2 isochrones, $a/R_\star$ constraint
$\log g$	$4.214^{+0.085}_{-0.015}$	Y^2 isochrones, $a/R_\star$ constraint
Mass ($M_\odot$)	$1.298^{+0.062}_{-0.098}$	Y^2 isochrones, $a/R_\star$ constraint
Radius ($R_\odot$).....	$1.474^{+0.042}_{-0.167}$	Y^2 isochrones, $a/R_\star$ constraint
$\log L_\star$ ($L_\odot$).....	$0.485^{+0.052}_{-0.134}$	Y^2 isochrones, $a/R_\star$ constraint
M_V	$3.54^{+0.36}_{-0.15}$	Y^2 isochrones, $a/R_\star$ constraint
Age (Gyr).....	$2.6^{+0.8}_{-1.4}$	Y^2 isochrones, $a/R_\star$ constraint

Based on the *Hipparcos* parallax ($\pi = 7.39 \pm 0.88$ mas), the apparent magnitude $V = 8.71 \pm 0.01$ (Droege et al. 2006), the SME temperature, and a bolometric correction of $\mathrm{BC}_V = -0.011 \pm 0.011$ mag (Flower 1996), the application of the Stefan-Boltzmann law yields a stellar radius of $R_\star = 1.84 \pm 0.24\ R_\odot$.

A more sophisticated approach to determine the stellar parameters uses stellar evolution models along with the observational constraints from spectroscopy. For this we used the Y^2 models by Yi et al. (2001) and Demarque et al. (2004), and explored a wide range of ages to find all models consistent with $T_{\rm eff}$, M_V, and [Fe/H] within the observational errors. Here $M_V = 3.05 \pm 0.26$ is the absolute visual magnitude, as calculated from V and the *Hipparcos* parallax. This procedure resulted in a mass and radius for the star of $M_\star = 1.42^{+0.10}_{-0.12}\ M_\odot$ and $R_\star = 1.85^{+0.31}_{-0.28}\ R_\odot$, and a best-fit age of $2.7^{+1.4}_{-0.6}$ Gyr. Other methods that rely on the *Hipparcos* parallax, such as the Padova stellar model grids[15] (Girardi et al. 2002), consistently yielded a stellar mass of $\sim$1.4 $M_\odot$ and stellar radius of $\sim$1.8 $R_\odot$.

If we do *not* rely on the *Hipparcos* parallax, and use $\log g$ as a proxy for luminosity (instead of M_V), then the Y^2 stellar evolution models yield a smaller stellar mass of $M_\star = 1.29^{+0.17}_{-0.12}\ M_\odot$, a radius of $R_\star = 1.46^{+0.36}_{-0.27}\ R_\odot$, and a best-fit age of $2.6^{+0.8}_{-2.5}$ Gyr. The surface gravity is a sensitive measure of the degree of evolution of the star, as is luminosity, and therefore has a very strong influence on the radius. However, $\log g$ is a notoriously difficult quantity to measure spectroscopically and is often strongly correlated with other spectroscopic parameters.

It has been pointed out by Sozzetti et al. (2007) that the normalized separation $a/R_\star$ can provide a much better constraint for stellar parameter determination than $\log g$. The $a/R_\star$ quantity can be determined directly from the photometric observations, without additional assumptions, and it is related to the density of the central star. As discussed below in § 6, an analytic fit to the FLWO 1.2 m light curve, taking into account an eccentric orbit, yielded $a/R_\star = 9.77^{+1.10}_{-0.02}$. Using this as a constraint, along with $T_{\rm eff}$ and [Fe/H], we obtained $M_\star = 1.30^{+0.06}_{-0.10}\ M_\odot$, $R_\star = 1.47^{+0.04}_{-0.17}\ R_\odot$, and an age of $2.6^{+0.8}_{-1.4}$ Gyr. The $\log g = 4.214^{+0.085}_{-0.015}$ derived this way is consistent with former value from SME.

As seen from the above discussion, there is an inconsistency between stellar parameters depending on whether the *Hipparcos* parallax is used or not. Methods relying on the parallax (Stefan-Boltzmann law, stellar evolution models with M_V constraint, etc.)

[15] At http://pleiadi.pd.astro.it.

favor a larger mass and radius ($\sim$1.4 $M_\odot$ and $\sim$1.8 $R_\odot$, respectively), whereas methods that do not rely on the parallax (stellar evolution models with $\log g$ or $a/R_\star$ constraint) point to smaller mass and radius ($\sim$1.3 $M_\odot$ and $\sim$1.46 $R_\odot$, respectively). We have chosen to rely on the $a/R_\star$ method, which yields considerably smaller uncertainties and a calculated transit duration that matches the observations. In addition, it implies an angular diameter for the star ($\phi = 0.127^{+0.021}_{-0.014}$ mas) that is in agreement with the more direct estimate of $\phi = 0.117 \pm 0.001$ mas from the near-infrared surface-brightness relation by Kervella et al. (2004). The latter estimate depends only on the measured $V - K_s$ color and apparent K_s magnitude (ignoring extinction) from 2MASS (Skrutskie et al. 2006), properly converted to the homogenized Bessell & Brett system for this application (following Carpenter 2001). We note that our results from the $a/R_\star$ method imply a somewhat smaller distance to HD 147506 than the one based on the *Hipparcos* parallax. The final adopted stellar parameters are listed in Table 2.

3.1. *Stellar Jitter*

Stars with significant rotation are known to exhibit excess scatter ("jitter") in their radial velocities (e.g., Wright 2005 and references therein), due to enhanced chromospheric activity and the associated surface inhomogeneities (spottedness). This jitter comes in addition to the internal errors in the measured velocities and could potentially be significant in our case. We note that after prewhitening the light curve with the transit component, we found no significant sinusoidal signal above 0.3 mmag amplitude. From this we conclude that there is no very significant spot activity on the star (in the observed 500 day window). In order to estimate the level of chromospheric activity in the star, we have derived an activity index from the Ca II H and K lines in our Keck spectra of $\log R'_{\rm HK} = -4.72 \pm 0.05$. For this value the calibration by Wright (2005) predicts velocity jitter ranging from 8 to 16 m s^{-1}. An earlier calibration by Saar et al. (1998), parameterized in terms of the projected rotational velocity, predicts a jitter level of up to 50 m s^{-1} for our measured $v \sin i$ of 20 km s^{-1}. A different calibration by the same authors in terms of $R'_{\rm HK}$ gives 20 m s^{-1}. An additional way to estimate the jitter is to compare HD 147506 to stars of the Lick Planet Search program (Cumming et al. 1999) that have similar properties ($0.4 < B - V < 0.5$, $v \sin i > 15$ km s^{-1}). There are four such stars (J. Johnson 2007, private communication), and their average jitter is 45 m s^{-1}. A more direct measure for the particular case of HD 147506 may be obtained from the multiple exposures we collected during a three-night Keck run in 2007 March. Ignoring the small velocity variations due to orbital motion during any given night, the overall scatter of these eight exposures relative to the nightly means is $\sim$20 m s^{-1}. This may be taken as an estimate of the jitter on short timescales, although it could be somewhat larger over the entire span of our observations. Altogether, it is reasonable to expect the jitter to be at least 10 m s^{-1}, and possibly around 30–50 m s^{-1} for this star.

4. SPECTROSCOPIC ORBITAL SOLUTION

We have three velocity data sets available for analysis (13 relative radial velocity measurements from Keck, 10 from Lick, and 53 measurements from the CfA DS), which are nominally on an absolute scale (Table 1). Given the potential effect of stellar jitter, we performed weighted Keplerian orbital solutions for a range of jitter values from 10 to 80 m s^{-1}, with 10 m s^{-1} steps. These jitter values were added in quadrature to all individual internal errors. We performed separate fits for the star orbited by a single planet, both with and without the CfA DS measurements, since these have errors ($\sim$600 m s^{-1}) significantly larger than Keck (5–9 m s^{-1}) or Lick (40–90 m s^{-1}). In all of these solutions we held the period and transit epoch fixed at the photometric values given earlier. The parameters adjusted are the velocity semiamplitude K, the eccentricity e, the longitude of periastron ω, the center-of-mass velocity for the Keck relative velocities γ, and offsets $\Delta v_{\rm KL}$, between Keck and Lick, and $\Delta v_{\rm KC}$, between Keck and CfA DS. The fitted parameters were found to be fairly insensitive to the level of jitter assumed. However, only for a jitter of $\sim$60 m s^{-1} (or $\sim$70 m s^{-1} when the CfA DS data are included) did the χ^2 approach values expected from the number of degrees of freedom. There are thus two possible conclusions: if we accept that HD 147506 has stellar jitter at the 60 m s^{-1} level, then a single-planet solution such as ours adequately describes our observations. If, on the other hand, the true jitter is much smaller ($\lesssim$20 m s^{-1}), then the extra scatter requires further explanation (see below). Our adopted orbital parameters for the simplest single-planet Keplerian solution are based only on the more precise Keck and Lick data, and assume that the jitter is 60 m s^{-1} (Table 3). The orbital fit is shown graphically in the top panel of Figure 2. In this figure, the zero point of phase is chosen to occur at the epoch of midtransit, $T_{\rm mid} = 2{,}454{,}212.8559$ (HJD). The most significant results are the large eccentricity ($e = 0.520 \pm 0.010$) and the large velocity semiamplitude ($K = 1011 \pm 38$ m s^{-1}, indicating a very massive companion). As we show in the next section (§ 5), the companion is a planet, i.e., HD 147506b, which we hereafter refer to as HAT-P-2b.

As a consistency check we also fitted the orbits by fixing only the period and leaving the transit epoch as a free parameter. We found that for all values of the stellar jitter the predicted time of transit as derived from the RV fit was consistent with the photometric ephemeris within the uncertainties. We also found that in these fits the orbital parameters were insensitive to the level of jitter and to whether or not the CfA DS data were included. The eccentricity values ranged from 0.51 to 0.53.

We note that the accuracy of the HAT-P-2 system parameters, notably the K velocity semiamplitude (i.e., the planetary mass), will profit from extensive high-precision radial velocity monitoring, since the current data set has limited phase coverage and the periastron passage is only covered by two Lick points that have precision inferior to the Keck data.[16]

4.1. *Solutions Involving Two Planets*

If we assume that the true stellar jitter is small, then the excess scatter in the RV fit could be explained by a third body in the system, i.e., a hypothetical HAT-P-2c. In addition, such a body could provide a natural dynamical explanation for the large eccentricity of HAT-P-2b at this relatively short period orbit. Preliminary two-planet orbital fits using all the data yielded solutions only significant at the 2 σ level, not compelling enough to consider as evidence for such a configuration. Additional RV measurements are needed to firmly establish or refute the existence of HAT-P-2c.

We also exploited the fact that the HATNet light curve has a unique time coverage and precision, and searched for signs of a second transit that might be due to another orbiting body around the host star. Successive box prewhitening based on the BLS spectrum and assuming trapezoidal-shape transits revealed no secondary transit deeper than the 0.1% level and period $\lesssim$10 days.

5. EXCLUDING BLEND SCENARIOS

As an initial test to explore the possibility that the photometric signal we detect is a false positive (blend) due to contamination from an unresolved eclipsing binary, we modeled the light curve

[16] Measurements made after the acceptance of this paper indeed point toward a somewhat smaller planetary mass, between 8 and 9 $M_{\rm J}$.

TABLE 3
Orbital Fit and Planetary Parameters for the HAT-P-2 System

Parameter	Value
Period (days)[a]	5.63341 ± 0.00013
$T_{\rm mid}$ (HJD)[a]	2,454,212.8559 ± 0.0007
Transit duration (days)	0.177 ± 0.002
Ingress duration (days)	0.012 ± 0.002
Stellar jitter (m s^{-1})[b]	60
γ (m s^{-1})[c]	−278 ± 20
K (m s^{-1})	1011 ± 38
ω (deg)	179.3 ± 3.6
e	0.520 ± 0.010
$T_{\rm peri}$ (HJD)	2,454,213.369 ± 0.041
$\Delta v_{\rm KL}$ (m s^{-1})	−380 ± 35
$\Delta v_{\rm KC}$ (km s^{-1})[d]	19.827 ± 0.087
$f(M)$ ($M_\odot$)	$(376 \pm 42) \times 10^{-9}$
$M_p \sin i$ ($M_{\rm J}$)	$7.56 \pm 0.28([M_\star + M_p]/M_\odot])^{2/3}$
$a_\star \sin i$ (km)	$(0.0669 \pm 0.0025) \times 10^6$
$a_{\rm rel}$ (AU)	0.0677 ± 0.0014
i_p (deg)	>84.6 (95% confidence)
M_p ($M_{\rm J}$)	9.04 ± 0.50
R_p ($R_{\rm J}$)	$0.982^{+0.038}_{-0.105}$
ρ_p (g cm^{-3})	$11.9^{+4.8}_{-1.6}$
g_p (m s^{-2})	227^{+44}_{-16}

[a] Fixed in the orbital fit.
[b] Adopted (see text).
[c] The γ velocity is not in an absolute reference frame.
[d] The offset between Keck and CfA DS is given for reference from a fit that includes all data sets, but does not affect our solution.

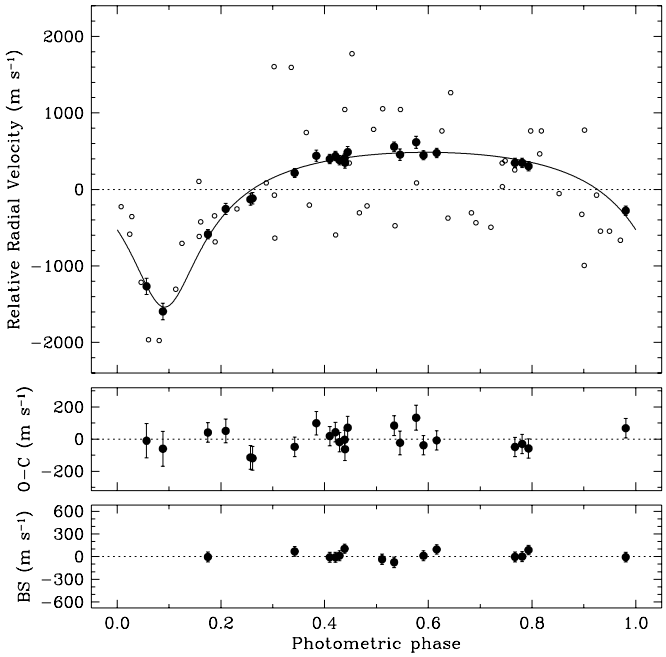

Fig. 2.—*Top*: RV measurements phased with the period of $P = 5.63341$ days. The zero point in phase corresponds to the epoch of midtransit. Large filled circles indicate Keck and Lick points. Small open circles denote CfA DS data (not used for the fit). Overlaid is the fit that was based only on the Keck and Lick data assuming 60 m s^{-1} stellar jitter. *Middle*: Residuals from the fit. *Bottom*: Line bisector spans on the same scale as in the top panel. No variation in the line bisectors is seen concomitant with that in the RVs, essentially confirming the planetary nature of the transiting object.

assuming that there are three coeval stars in the system, as described by Torres et al. (2004). We were indeed able to reproduce the observed light curve with a configuration in which the brighter object is accompanied by a slightly smaller F star that is in turn being eclipsed by a late-type M dwarf. However, the predicted relative brightness of the two brighter objects at optical wavelengths would be ∼0.58, and this would have been easily detected in our spectra. This configuration can thus be ruled out.

The reality of the velocity variations was tested by carefully examining the spectral line bisectors of the star in our more numerous Keck spectra. If the velocity changes measured are due only to distortions in the line profiles arising from contamination of the spectrum by the presence of a binary with a period of 5.63 days, we would expect the bisector spans (which measure line asymmetry) to vary with this period and with an amplitude similar to the velocities (see, e.g., Queloz et al. 2001; Torres et al. 2005). The bisector spans were computed from the cross-correlation function averaged over 15 spectral orders blueward of 5000 Å and unaffected by the iodine lines, which is representative of the average spectral line profile of the star. The cross-correlations were performed against a synthetic spectrum matching the effective temperature, surface gravity, and rotational broadening of the star as determined from the SME analysis. As shown in Figure 2, while the measured velocities exhibit significant variation as a function of phase (*top panel*), the bisector spans are essentially constant within the errors (*bottom panel*). Therefore, this analysis rules out a blend scenario and confirms that the orbiting body is indeed a planet.

6. PLANETARY PARAMETERS

For a precise determination of the physical properties of HAT-P-2b we have modeled the FLWO 1.2 m Sloan z-band photometric data shown in Figure 1. The model is an eccentric Keplerian orbit of a star and planet, thus accounting for the nonuniform speed of the planet and the reflex motion of the star. Outside of transits, the model flux is unity. During transits, the model flux is computed using the formalism of Mandel & Agol (2002), which provides an analytic approximation of the flux of a limb-darkened star that is being eclipsed. The free parameters were the midtransit time $T_{\rm mid}$, the radius ratio $R_p/R_\star$, the orbital inclination i, and the scale parameter $a/R_\star$, where a is the semimajor axis of the relative orbit. The latter parameter is determined by the timescales of the transit (the total duration and the partial-transit duration) and is related to the mean density of the star (see § 3). The orbital period, eccentricity, and argument of pericenter were fixed at the values determined previously by fitting the radial velocity data. The limb-darkening law was assumed to be quadratic, with coefficients taken from Claret (2004).

To solve for the parameters and their uncertainties, we used a Markov chain Monte Carlo algorithm that has been used extensively for modeling other transits (see, e.g., Winn et al. 2007; Holman et al. 2007). This algorithm determines the a posteriori probability distribution for each parameter, assuming independent ("white") Gaussian noise in the photometric data. However, we found that there are indeed correlated errors. Following Gillon et al. (2006), we estimated the red noise σ_r via the equation

$$\sigma_r^2 = \frac{\sigma_N^2 - \sigma_1^2/N}{1 - 1/N}, \quad (1)$$

where σ_1 is the standard deviation of the out-of-transit flux of the original (unbinned) light curve, σ_N is the standard deviation of the light curve after binning into groups of N data points, and $N = 40$ corresponds to a binning duration of 20 minutes, which is the ingress/egress timescale that is critical for parameter estimation. With white noise only, $\sigma_N = \sigma_1/\sqrt{N}$ and $\sigma_r = 0$. We added

σ_r in quadrature to the error bar of each point, effectively inflating the error bars by a factor of 1.25.

The result for the radius ratio is $R_p/R_\star = 0.0684 \pm 0.0009$, and for the scale parameter $a/R_\star = 9.77^{+1.10}_{-0.02}$. The a posteriori distribution for $a/R_\star$ is very asymmetric because the transit is consistent with being equatorial: $i > 84.6^\circ$, with 95% confidence. We confirmed that these uncertainties are dominated by the photometric errors, rather than by the covariances with the orbital parameters e, ω, and P, and hence we were justified in fixing those orbital parameters at constant values. Based on the inclination, the mass of the star (Table 2), and the orbital parameters (Table 3), the planet mass is then $9.04 \pm 0.50\ M_J$. Based on the radius of the star (Table 2) and the above $R_p/R_\star$ determination, the radius of the planet is $R_p = 0.982^{+0.038}_{-0.105}\ R_J$. These properties are summarized in Table 3.

7. DISCUSSION

In comparison with the other 18 previously known transiting exoplanets, HAT-P-2b is quite remarkable (Figs. 3 and 4). Its mass of $9.04 \pm 0.50\ M_J$ is $\sim$5 times greater than any of these 18 other exoplanets. Its mean density $\rho = 11.9^{+4.8}_{-1.6}$ g cm^{-3} is $\sim$9 times that of the densest known exoplanet (OGLE-TR-113b, $\rho = 1.35$ g cm^{-3}) and indeed greater than that of the rocky planets of the solar system ($\rho = 5.5$ g cm^{-3}). Its surface gravity of 227^{+44}_{-16} m s^{-2} is 7 times that of any of the previously known TEPs and 30 times that of HAT-P-1b (Fig. 4).

We may compare the mass and radius for HAT-P-2b with evolutionary models, including irradiation, as recently presented by FMB07. Given the inferred stellar luminosity (Table 2) and the time-integral of the insolation over an entire period (taking into account the orbital parameters, notably e and a_{rel}), the equivalent semimajor axis a_{eq} for the same amount of irradiation if the central star were solar is 0.036 AU. At that separation, FMB07 find for a pure hydrogen/helium planet of mass 9 M_J and age of 4.5 Gyr a planetary radius about 1.099 R_J. A 100 $M_\oplus$ core has a negligible effect on the radius (yielding 1.068 R_J), which is not surprising, since the mass of such a core is only a few percent of the total mass. For younger ages, of 1 and 0.3 Gyr, the radii are even larger:

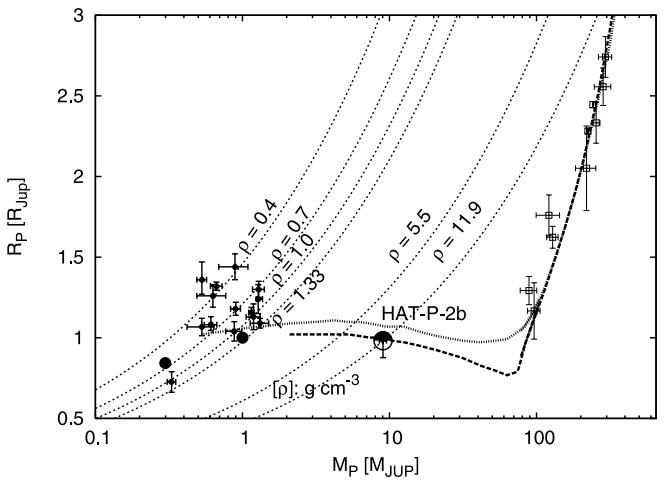

FIG. 3.—Mass-radius diagram of known TEPs (from http://www.exoplanet.eu and references therein), Jupiter and Saturn (*large filled circles*), and low-mass stars from Beatty et al. (2007). HAT-P-2b is an intermediate-mass object that is still in the planetary regime (well below 13 M_J). Overlaid are equidensity lines (labeled), Baraffe et al. (1998) (stellar) and Baraffe et al. (2003) (zero insolation planetary) isochrones for ages of 0.5 Gyr (*thick dotted line*) and 5 Gyr (*thick dashed-line*), respectively. [*See the electronic edition of the Journal for a color version of this figure.*]

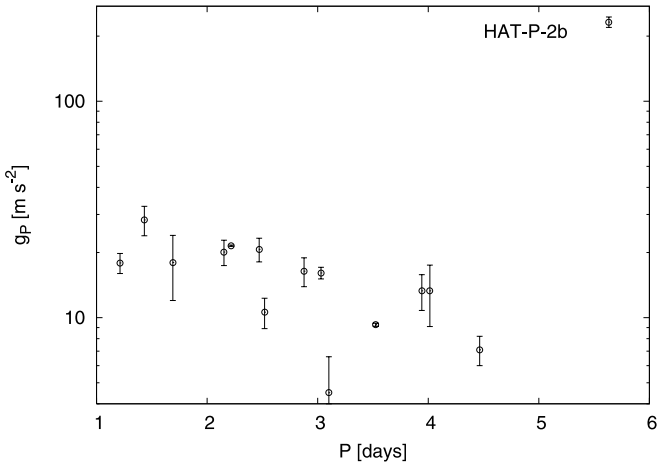

FIG. 4.—Surface gravity of TEPs as a function of orbital period. Data taken from Southworth et al. (2007) with the exception of HAT-P-2b. This object is clearly not obeying the suspected correlation of g_p and P for "Jupiter-mass" objects.

1.159 and 1.22 R_J, respectively, for coreless models. Our observed radius of 0.982 R_J is smaller than any of the above values (4.5, 1, 0.3 Gyr, with or without the 100 $M_\oplus$ core). Since the 1 σ positive error bar on our radius determination is 0.038 R_J, the inconsistency is only marginal (at the 3–5 σ level). Nevertheless, the observed radius favors either greater age or bigger core size, or both. Given the age of the host star (2.6 Gyr; Table 2), the greater age is an unlikely explanation. The required core size for this mass and radius according to FMB07 would be 300 $M_\oplus$, an amount of icy and rocky material that may be hard to account for. We note that using the alternate (and not favored) stellar radius of $R_\star \approx 1.84\ R_\odot$ that relies on methods based on the *Hipparcos* parallax (§ 3), the planetary radius would be $R_p \approx 1.2\ R_J$. This is broadly consistent with young and coreless models of FMB07.

Figure 3 also shows a theoretical mass-radius relation for objects ranging from gas giant planets to stars (Baraffe et al. 1998, 2003). Note that HAT-P-2b falls on the relation connecting giant planets to brown dwarfs to stars. It thus appears to be intermediate in its properties, between Jupiter-like planets and more massive objects such as brown dwarfs or even low-mass stars. According to theories, stars with mass $\gtrsim 0.2\ M_\odot$ have a core, in which internal pressure is dominated by classical gas (ions and electrons), and the $R \propto M$ radius–mass relation holds in hydrostatic equilibrium (for a review and details on the following relations, see, e.g., Chabrier et al. 2000). Below $\sim 0.075\ M_\odot$ (80 M_J) mass, however, the equation of state in the core becomes dominated by degenerate electron gas ($R \propto M^{-1/3}$ for full degeneracy), yielding an expected minimum in the mass–radius relationship (around 73 M_J). Below this mass, the partial degeneracy of the object and the classical ($R \propto M^{1/3}$) Coulomb pressure together yield an almost constant radius ($R \propto M^{-1/8}$). HAT-P-2b is a demonstration of this well-known phenomenon. (The approximate relation breaks below $M \sim 4\ M_J$, where the degeneracy saturates, and a classical mass-radius behavior is recovered).

Compared to the other 18 known transiting planets, HAT-P-2b is also unique in having an orbit with remarkably high eccentricity. The primary question is how such an eccentricity was created in the first place. One possible explanation could be that the planet was scattered inward from a larger orbit, acquiring a high eccentricity in the process (Ford & Rasio 2007; Chatterjee et al. 2007). If so, then the scattering event might have caused its new orbital plane to be inclined relative to the plane of the original disk, and

hence out of the equatorial plane of the parent star (e.g., Fabrycky & Tremaine 2007). This angle between these two planes should be readily measurable from the Rossiter-McLaughlin effect (Winn et al. 2005). Indeed, the star HD 147506 is an ideal subject for studying this effect, because its rapid rotation should lead to a relatively large Rossiter-McLaughlin signal.

There are a number of other interesting issues related to the high eccentricity of HAT-P-2b. During its 5.63 day orbit, the insolation reaching the planet's surface varies by a factor of 9. Assuming an albedo of 0.1 (Rowe et al. 2006) and complete redistribution of insolation energy over the surface of the planet, the equilibrium temperature varies from about 2150 K at periastron to 1240 K at apastron. This would have a major influence on atmospheric dynamics and photochemistry.

It is interesting to compare the properties of the HAT-P-2 system with the τ Boo system, which—as already noted—harbors a close-in planet with minimum mass $M_p \sin i = 3.9\,M_J$. Similarities of the two parent stars include the nearly identical masses, effective temperature, and rapid rotation, although τ Boo, with $[\mathrm{Fe/H}] = +0.28$, is somewhat more metal-rich than HD 147506, with $[\mathrm{Fe/H}] = +0.12$. A striking difference is that, while the orbital eccentricity of HAT-P-2b is 0.5, the eccentricity of τ Boo b is not measurably different from zero. However, τ Boo b's orbital period, 3.3 days, is almost half that of HAT-P-2b. A large fraction of close-in planets with $5 < P < 10$ days have significant eccentricities ($0.1 < e < 0.3$), although not as large as HAT-P-2b. For discussion on the eccentricity distribution, see Juric & Tremaine (2007). As circularization timescales are thought to be very steep functions of the orbital semimajor axis (Terquem et al. 1998), one could then argue that HAT-P-2b's large value of e is due to either the fact that the planet's orbit is not yet circularized (while τ Boo b's instead is) to the presence of a second planet in the HAT-P-2 system, or to rather different formation/migration scenarios altogether.

HD 147506, with visual magnitude 8.71, is the fourth brightest among the known stars harboring transiting planets. Therefore, it has special interest because of the possibilities for follow-up with large space- or ground-based telescopes.

Operation of the HATNet project is funded in part by NASA grant NNG04GN74G. Work by G. Á. B. was supported by NASA through Hubble Fellowship Grant HST-HF-01170.01-A. G. K. wishes to offer thanks for support from the Hungarian Scientific Research Foundation (OTKA) grant K-60750. We acknowledge partial support from the Kepler Mission under NASA Cooperative Agreement NCC2-1390 (PI: D. W. L.). G. T. acknowledges partial support from NASA Origins grant NNG04LG89G. T. M. thanks the Israel Science Foundation for a support through grant 03/233. D. A. F. is a Cottrell Science Scholar of Research Corporation and acknowledges support from NASA grant NNG05G164G. We would like to thank Joel Hartman (CfA), Gil Esquerdo (CfA), and Ron Dantowitz and Marek Kozubal (Clay Center) for their efforts to observe HAT-P-2b in transit, and Howard Isaacson (San Francisco State University) for obtaining spectra at Lick Observatory. We wish to thank Amit Moran for his help in the observations with the Wise HAT telescope. We owe special thanks to the directors and staff of FLWO, SMA, and the Wise Observatory for supporting the operation of HATNet and WHAT. We would also like to thank the anonymous referee for the useful suggestions that improved this paper.

REFERENCES

Bakos, G. Á., Lázár, J., Papp, I., Sári, P., & Green, E. M. 2002, PASP, 114, 974
Bakos, G. Á., Noyes, R. W., Kovács, G., Stanek, K. Z., Sasselov, D. D., & Domsa, I. 2004, PASP, 116, 266
Bakos, G. Á., et al. 2007, ApJ, 656, 552
Baraffe, I., Chabrier, G., Allard, F., & Hauschildt, P. H. 1998, A&A, 337, 403
Baraffe, I., Chabrier, G., Barman, T. S., Allard, F., & Hauschildt, P. H. 2003, A&A, 402, 701
Beatty, T. G., et al. 2007, ApJ, 663, 573
Bodenheimer, P., Laughlin, G., & Lin, D. N. C. 2003, ApJ, 592, 555
Burrows, A., et al. 1997, ApJ, 491, 856
Butler, R. P., Marcy, G. W., Williams, E., Hauser, H., & Shirts, P. 1997, ApJ, 474, L115
Carpenter, J. M. 2001, AJ, 121, 2851
Casagrande, L., Portinari, L., & Flynn, C. 2006, MNRAS, 373, 13
Chabrier, G., Baraffe, I., Allard, F., & Hauschildt, P. 2000, ApJ, 542, L119
Chatterjee, S., Ford, E. B., & Rasio, F. A. 2007, ApJ, submitted (astro-ph/0703166)
Claret, A. 2004, A&A, 428, 1001
Cumming, A., Marcy, G. W., & Butler, R. P. 1999, ApJ, 526, 890
Demarque, P., Woo, J.-H., Kim, Y.-C., & Yi, S. K. 2004, ApJS, 155, 667
Droege, T. F., Richmond, M. W., & Sallman, M. 2006, PASP, 118, 1666
Fabrycky, D., & Tremaine, S. 2007, ApJ, 669, 1298
Flower, P. J. 1996, ApJ, 469, 355
Ford, E. B., & Rasio, F. A. 2007, ApJ, submitted (astro-ph/0703163)
Fortney, J. J., Marley, M. S., & Barnes, J. W. 2007, ApJ, 659, 1661
Gillon, M., Pont, F., Moutou, C., Bouchy, F., Courbin, F., Sohy, S., & Magain, P. 2006, A&A, 459, 249
Girardi, L., et al. 2002, A&A, 391, 195
Guillot, T., & Showman, A. P. 2002, A&A, 385, 156
Holman, M. J., et al. 2007, ApJ, 664, 1185
Juric, M., & Tremaine, S. 2007, ApJ, submitted (astro-ph/0703160)
Kervella, P., Thévenin, Di Folco, E., & Ségransan, D. 2004, A&A, 426, 297
Kovács, G., Bakos, G. Á., & Noyes, R. W. 2005, MNRAS, 356, 557
Kovács, G., Zucker, S., & Mazeh, T. 2002, A&A, 391, 369
Latham, D. W. 1992, in IAU Colloq. 135, Complementary Approaches to Double and Multiple Star Research, ed. H. A. McAlister & W. I. Hartkopf (ASP Conf. Ser. 32; San Francisco: ASP), 110
Laughlin, G., Wolf, A., Vanmunster, T., Bodenheimer, P., Fischer, D., Marcy, G., Butler, P., & Vogt, S. 2005, ApJ, 621, 1072
Mandel, K., & Agol, E. 2002, ApJ, 580, L171
Masana, E., Jordi, C., & Ribas, I. 2006, A&A, 450, 735
Pál, A., & Bakos, G. Á. 2006, PASP, 118, 1474
Perryman, M. A. C., et al. 1997, A&A, 323, L49
Queloz, D., et al. 2001, A&A, 379, 279
Ramírez, I., & Meléndez, J. 2005, ApJ, 626, 465
Rowe, J. F., et al. 2006, ApJ, 646, 1241
Saar, S. H., Butler, R. P., & Marcy, G. W. 1998, ApJ, 498, L153
Sato, B., et al. 2005, ApJ, 633, 465
Shporer, A., Mazeh, T., Moran, A., Bakos, G. Á., Kovacs, G., & Mashal, E. 2006, Tenth Anniversary of 51 Peg-b: Status of and Prospects for Hot Jupiter Studies, ed. L. Arnold, F. Bouchy, & C. Moutou (Paris: Frontier Group), 196
Skrutskie, M. F., et al. 2006, AJ, 131, 1163
Southworth, J., Wheatley, P. J., & Sams, G. 2007, MNRAS, 379, L11
Sozzetti, A., Torres, G., Charbonneau, D., Latham, D. W., Holman, M. J., Winn, J. N., Laird, J. B., & O'Donovan, F. T. 2007, ApJ, 664, 1190
Terquem, C., Papaloizou, J. C. B., Nelson, R. P., & Lin, D. N. C. 1998, ApJ, 502, 788
Torres, G., Konacki, M., Sasselov, D. D., & Jha, S. 2004, ApJ, 609, 1071
———. 2005, ApJ, 619, 558
Valenti, J. A., & Fischer, D. A. 2005, ApJS, 159, 141
Valenti, J. A., & Piskunov, N. 1996, A&AS, 118, 595
Vogt, S. S. 1987, PASP, 99, 1214
Vogt, S. S., et al. 1994, Proc. SPIE, 2198, 362
Winn, J. N., Holman, M. J., & Fuentes, C. I. 2007, AJ, 133, 11
Winn, J. N., et al. 2005, ApJ, 631, 1215
Wright, J. T. 2005, PASP, 117, 657
Wright, J. T., et al. 2007, ApJ, 657, 533
Yi, S. K., Demarque, P., Kim, Y.-C., Lee, Y.-W., Ree, C. H., Lejeune, T., & Barnes, S. 2001, ApJS, 136, 417